

Nickel surface anodic oxidation and electrocatalysis of oxygen evolution

K. Juodkazis · J. Juodkazytė · R. Vilkauskaitė · V. Jasulaitienė

Received: 3 October 2007 / Revised: 12 November 2007 / Accepted: 26 November 2007 / Published online: 10 January 2008
© Springer-Verlag 2007

Abstract The processes of nickel surface anodic oxidation taking place within the range of potentials preceding oxygen evolution reaction (OER) in the solutions of 1 M KOH, 0.5 M K₂SO₄, and 0.5 M H₂SO₄ have been analyzed in the present paper. Metallic nickel, thermally oxidized nickel, and black nickel coating were used as Ni electrodes. The methods of cyclic voltammetry and X-ray photoelectron spectroscopy were employed. The study was undertaken with a view to find the evidence of peroxide-type nickel surface compounds formation in the course of OER on the Ni electrode surface. On the basis of experimental results and literature data, it has been suggested that in alkaline solution at $E \approx 1.5$ V (RHE) reversible electrochemical formation of Ni(IV) peroxide takes place according to the reaction as follows: $\text{NiO}(\text{OH})_2 + 2\text{OH}^- \leftrightarrow \text{NiOO}_2 + 2\text{H}_2\text{O} + 2\text{e}^-$. This reaction accounts for both the underpotential (with respect to $E_{\text{H}_2\text{O}_2/\text{H}_2\text{O}}^0 = 1.77$ V) formation of O₂ from NiOO₂ peroxide and also small experimental values of $dE/d\lg i$ slope (<60 mV) at low anodic current densities, which are characteristic for the two-electron transfer process. It has been inferred that the composition of the γ -NiOOH phase, indicated in the Bode and revised Pourbaix diagrams, should be $\sim 5/6$ NiOOH + $\sim 1/6$ NiOO₂. The schemes demonstrating potential-dependent transitions between Ni surface oxygen compounds are presented, and the electrocatalytic mechanisms of OER in alkaline, acid, and neutral medium have been proposed.

Keywords Nickel · Surface · Oxidation · Peroxide · Oxygen evolution reaction

Introduction

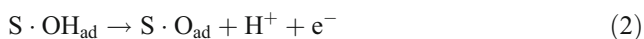
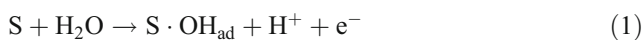
Metal oxides and their mixtures are widely used as catalysts and electrocatalysts in various technologically important processes [1–4]. Among such processes, the oxidation of water molecules to molecular oxygen (oxygen evolution reaction [OER]) plays an important role. The survey of recent relevant literature shows that up till now the intensive search for technologically effective, i.e., efficient, low cost, chemically stable anodes for OER is going on [5–13]. One of the challenges is seawater electrolysis where the main problem consists in the prevention of Cl₂ formation so as to receive pure H₂ and O₂ gases [14].

Traditionally, platinum is used for oxygen evolution in acidic medium, whereas in the alkaline one, nickel electrodes are employed. In fact, OER takes place on the electrode coated with metal oxides, which form on the electrode surface as the result of metal anodic oxidation before the beginning of OER. Among oxide electrodes, oxides of nickel, cobalt, and iron [8, 10–12, 15–17] are efficient for OER in alkaline medium. IrO₂ with or without RuO₂ exhibits best performance in acid and other solutions [1, 2, 6, 18]. Oxide electrodes are usually prepared in the form of coatings on conducting, chemically inert substrates like Ti, corrosion resistant alloys or carbon [5, 6].

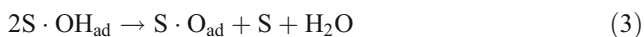
The mechanism of the oxygen evolution process on the surface of various metals and their oxides has been investigated for many years [1–3, 5, 8, 19–25]. Despite the fact that every instance of OER on the certain electrode surface is individual, it is almost generally accepted that the process goes through the main stages of adsorbed or

K. Juodkazis (✉) · J. Juodkazytė · R. Vilkauskaitė · V. Jasulaitienė
Institute of Chemistry,
A. Goštauto 9,
LT-01108 Vilnius, Lithuania
e-mail: kesjuod@ktl.mii.lt

chemisorbed OH_{ad} radicals and O_{ad} atoms formation as described below:



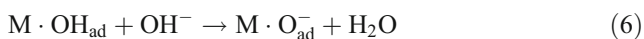
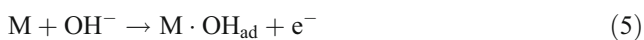
or



and



where S denotes the active site on the electrode surface [1, 2, 8]. O_{ad}^- has also been suggested as the possible intermediate in O_{ad} formation according to the scheme [7]:



where M denotes the surface site. Hence, Eqs. 1, 2, 3, 4, 5, 6, 7, and 8 do not reflect specific surface chemical or electrochemical processes; they just characterize the way of O_2 molecule formation. However, the above-described way (Eqs. 4 or 8) is not the only possible way [5, 26]. More realistic seems the way of molecular oxygen formation through the intermediate stage of adsorbed or chemisorbed peroxide ion $(\text{O}_2^-)_{\text{ad}}$ formation, i.e., via the H_2O_2 channel [26]. The possibility of adsorbed peroxide intermediate $\text{S}-\text{H}_2\text{O}_2$ formation from OH radicals has been proposed by Bockris and Otagawa [27]. Thermodynamically, the oxidation of water molecules to H_2O_2 and subsequently to O_2 is possible at $E \approx 1.8$ V because $E_{\text{H}_2\text{O}_2/\text{H}_2\text{O}}^0 = 1.77$ V and $E_{\text{O}_2/\text{H}_2\text{O}_2}^0 = 0.68$ V [28], whereas the oxidation of H_2O to OH radicals and O atoms requires significantly higher anodic potential values, i.e., $E_{\text{OH}/\text{H}_2\text{O}}^0 = 2.8$ V and $E_{\text{O}_2/\text{H}_2\text{O}}^0 = 2.4$ V [28].

The surface on which O_2 evolution process is most easy in both acid and alkaline solutions is that of ruthenium, or more precisely, the RuO_2 electrode where OER takes place at ~ 1.4 V (RHE) [2]. In the case of the IrO_2 electrode, the OER takes place at ~ 1.5 V (RHE) as it also does on the nickel electrode in the alkaline medium. The experimental E_{OER} values indicated are considerably more positive than $E_{\text{O}_2/2\text{H}_2\text{O}}^0 = 1.23$ V but considerably more negative than $E_{\text{H}_2\text{O}_2/\text{H}_2\text{O}}^0 = 1.77$ V. So the oxidation of the H_2O mole-

cules to O_2 in the case of oxides indicated takes place at overpotential with respect to $E_{\text{O}_2/2\text{H}_2\text{O}}^0$. However, if the process goes through the intermediate stage of adsorbed peroxide ion $(\text{O}_2^-)_{\text{ad}}$ formation, it would follow that OER takes place at underpotential, which is due to the possibility of intermediate surface peroxide formation.

The processes of nickel anodic oxidation and redox transitions between various nickel oxide forms, surface state, and composition of oxides have been widely and thoroughly investigated [15, 16, 19, 20, 25, 30–39]. One can say that presently the reasons of nickel passivation in acid and alkaline medium in the range of potentials preceding OER are identified. In recent studies [36, 40], it has been suggested that nickel is passivated by several molecular layers of nickel oxide NiO lying directly on the metal surface and covered with a compact layer of $\text{Ni}(\text{OH})_2$ hydroxide staying in contact with solution. However, the changes in nickel electrode surface state in the oxygen evolution region are not so well understood. Structurally, the following phases of nickel oxide are discerned: α -Ni(OH)₂, β -Ni(OH)₂, β -NiOOH, and γ -NiOOH [38, 39], but the precise composition of these phases and the conditions of their formation on the nickel electrode surface are not clearly defined so far. It is believed that the γ -NiOOH phase is involved in OER in alkaline medium. γ -NiOOH is considered to consist of mixed Ni^{4+} and Ni^{2+} oxides with average nickel oxidation state being ~ 3.6 [38, 39]. It is not clear, however, how this phase participates in OER and what is the mechanism of this process.

In the present study, the changes in the surface state of nickel electrode in acid, neutral, and alkaline solutions in the E range preceding oxygen evolution have been analyzed with a view to verify the assumption regarding the formation of peroxide-type compounds on the electrode surface. The OER on nickel, thermally treated nickel, and black nickel deposit electrodes has been investigated.

Experimental

Electrochemical measurements

The voltammetric measurements were performed using the PI-50-1.1 potentiostat with a PR-8 programming device (Russia) connected to a personal computer. A conventional ~ 25 cm³ glass cell with separate working, counter, and reference electrode compartments was used. Pure Pt (99.99%) plate served as a counter electrode. Hydrogen electrode in a working solution (RHE) was used as reference. The potential values in the text are referred to the RHE scale, which makes it easy to compare the results obtained in the case of solutions with various pH. The relationship between the two scales is given by: $E_{\text{RHE}} =$

$E_{\text{SHE}} - 0.059$ pH. All current density values given in the text refer to the apparent area of the working electrode, i.e., 1.0 cm^2 .

Metallic nickel, thermally treated nickel, and black nickel coating were used as working electrodes. Nickel electrode was cut from pure Ni ($\geq 99.99\%$) sheet 0.1 mm thick. Before measurements, the electrode was polished with fine emery paper, degreased with fine-grained pulp of $\text{MgO} + \text{Ca}(\text{OH})_2$, washed, and activated for 30 s in $0.5 \text{ M H}_2\text{SO}_4$. To prepare thermally treated nickel, the Ni plate was heated at $400 \text{ }^\circ\text{C}$ for $\sim 30 \text{ min}$ and subjected to no further treatment before measurements. Black nickel coating (0.1 – $0.2 \text{ }\mu\text{m}$ thick) was deposited on the Ni plate initially coated with thin ($0.05 \text{ }\mu\text{m}$) nickel underlayer. The latter was deposited from strongly acid chloride electrolyte containing $250 \text{ g dm}^{-3} \text{ NiCl}_2 \cdot 6\text{H}_2\text{O}$ and $20 \text{ cm}^3 \text{ dm}^{-3}$ concentrated HCl; at $i_c = 5 \text{ A dm}^{-2}$ and $20 \text{ }^\circ\text{C}$. Black nickel coating was deposited from industrially used electrolyte consisting of $25 \text{ g dm}^{-3} \text{ NiSO}_4 \cdot 7\text{H}_2\text{O}$, $30 \text{ g dm}^{-3} \text{ Na}_2\text{SO}_4$, $20 \text{ g dm}^{-3} \text{ H}_3\text{BO}_3$, and $100 \text{ cm}^3 \text{ dm}^{-3}$ additive, containing organic ligand and KSCN, pH 6.0 – 7.0 , 20 – $30 \text{ }^\circ\text{C}$, $i_c = 1.0 \text{ A dm}^{-2}$.

Chemicals of analytical grade and triply distilled water were used to prepare the solutions. When necessary, the solutions were deaerated before measurements by bubbling pure argon through them for approximately 30 min . Argon was also used to maintain the inert atmosphere over the solutions during the measurements. All experiments were carried out at room temperature ($20 \text{ }^\circ\text{C}$).

XPS measurements

The composition of black nickel coatings was analyzed using X-ray photoelectron spectroscopy (XPS). The spectra were recorded with the spectrometer “ESCALAB MK II” (VG Scientific, Great Britain) using X-radiation of MgK_α ($1,253.6 \text{ eV}$, pass energy of 20 eV). The spectrometer had a base pressure of $5 \times 10^{-8} \text{ Torr}$ in the analyzer chamber and $2 \times 10^{-8} \text{ Torr}$ in the sample preparation chamber where Ar^+ ion bombardment was performed. For sputter etching, the argon gas pressure was maintained at $6 \times 10^{-5} \text{ Torr}$ and the

ion gun was operated at 2 kV . The approximate rate of nickel phase etching is $\sim 0.3 \text{ nm min}^{-1} \mu\text{A}^{-1}$. Elemental analysis of coatings and the valence state of Ni $2p_{3/2}$, O $1s$, C $1s$, S $2p$ was studied using the XPS method. The quantitative elemental analysis was done by estimating peak areas and taking into account empirical sensitivity factors for each element [41] and then the spectra recorded were compared to the standard spectra [42, 43]. The binding energies were calibrated with respect to the C $1s$ electron peak at 284.6 eV due to residual pump oil on the sample surface. No less than five spectra were recorded for every element. A maximum accuracy of the method was at $0.1 \text{ at.}\%$. Standard and experimentally found binding energy values for the $\text{Ni}(\text{OH})_2$, NiO, and NiS compounds are given in Table 1 [42, 43]. A standard program was used for data processing (XPS spectra were treated by a Shirley-type background subtraction and fitted with mixed Gaussian–Lorentzian functions).

Results and discussion

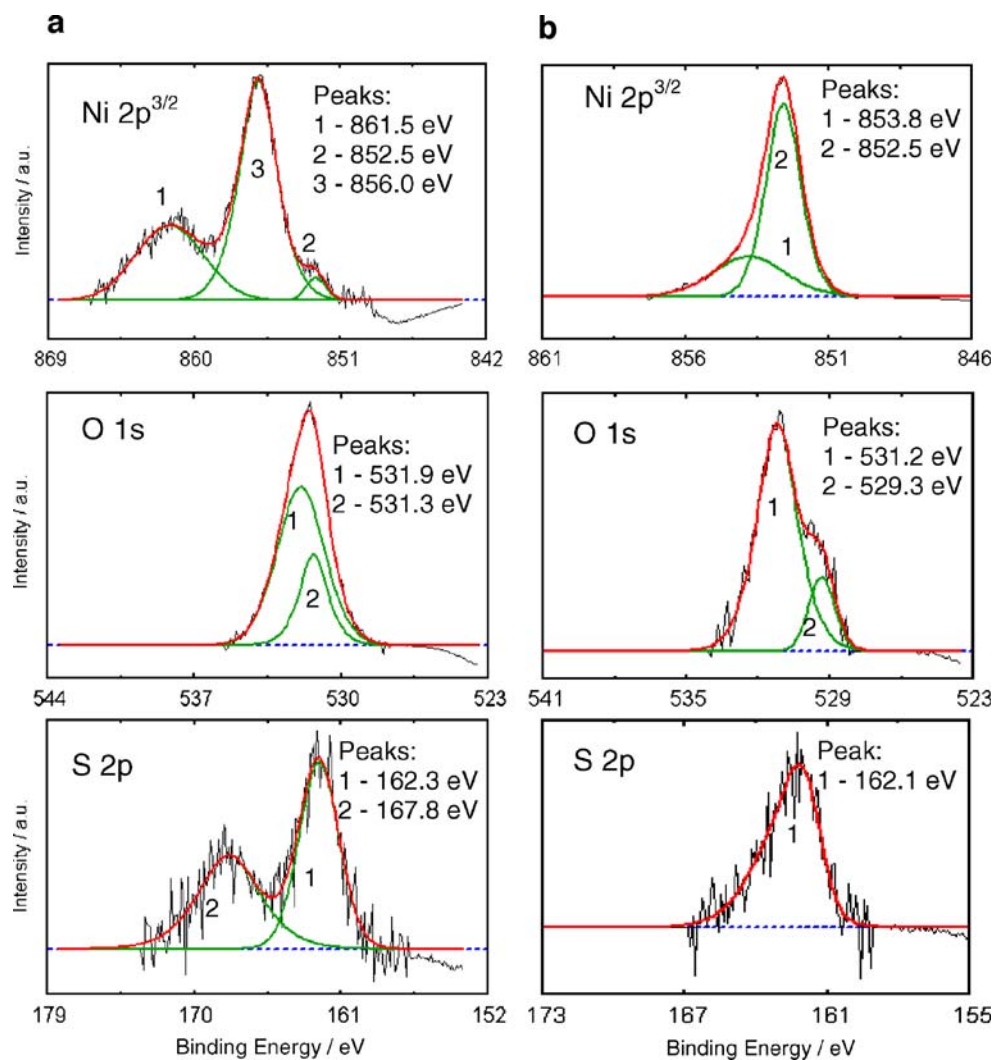
XPS spectra characterizing the surface state of black nickel coating as-deposited and after argon etching ($100 \mu\text{A}$, 3 min) are presented in Fig. 1a and b, respectively. Analysis of the spectra, standard binding energy values given in Table 1, and the data of surface elemental composition clearly show that the main component of the as-deposited black nickel coating surface is $\text{Ni}(\text{OH})_2$ (Fig. 1a). In addition, small amounts of C and S were found in the coating, the source of which might be the KSCN component present in the black nickel-plating electrolyte. After the partial removal of the surface layer ($\sim 0.09 \mu\text{m}$ thick) by means of argon etching (Fig. 1b), the amount of Ni increased significantly and the prevailing surface compound was found to be NiO. Another possible constituent of the coating may be NiS.

Cyclic voltammograms in Fig. 2 illustrate the processes of nickel surface anodic oxidation and cathodic reduction of the anodic reaction products in the solutions of 1 M KOH , $0.5 \text{ M K}_2\text{SO}_4$, and $0.5 \text{ M H}_2\text{SO}_4$. In alkaline and neutral

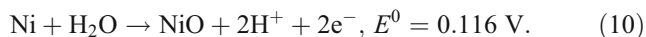
Table 1 Standard and experimentally found binding energies of nickel compounds [42, 43]

Compound	Standard and experimental binding energy (eV)					
	Ni $2p_{3/2}$		O $1s$		S $2p$	
	Standard	Exp.	Standard	Exp.	Standard	Exp.
$\text{Ni}(\text{OH})_2$	855.9	856.0	530.8–531.7	531.9 531.3 531.2		
NiO	854.4	853.8	529.3–530.7	529.3		
NiS	852.8–853.2	852.5			162.1–162.8	162.3 162.1

Fig. 1 XPS spectra of black nickel coating surface: **a** as-deposited; **b** after argon etching for 3 min at 100 μ A



solutions, Ni should behave like electropositive metal because the first anodic process according to Pourbaix [28] should be the oxidation of nickel to slightly soluble hydroxide $\text{Ni}(\text{OH})_2$ or oxide NiO according to the following reactions:



The thermodynamic probability of $\text{Ni}(\text{OH})_2$ and NiO formation is practically the same. One can see that in the case of alkaline and neutral solutions (Fig. 2, curves 1 and 2), hydrogen evolution reaction takes place at $E < 0$, i.e., at slight overvoltage of 50 to 100 mV. Judging from curves 1 and 2 (Fig. 2), the anodic oxidation of nickel in the case of the active state of the Ni electrode surface, i.e., after the

activation with H_2 , begins at the potentials more negative ($E < 0$) than the thermodynamic values and is reflected in voltammograms as wide anodic current peaks spanning the range of potentials up to 0.7–0.8 V. Anodic charges corresponding to these peaks are $Q_a^{(1)} \approx 4.8 \text{ mC cm}^{-2}$ and $Q_a^{(2)} \approx 3.2 \text{ mC cm}^{-2}$, respectively. Considering the roughness factor f of the mechanically polished Ni electrode surface, which should be in the range between 2 and 3, and the charge required to oxidize the monolayer of nickel atoms to the Ni^{2+} state, which is $\sim 0.4 \text{ mC cm}^{-2}$ in the case of ideally smooth surface ($f=1$), the above-indicated values of Q_a correspond to the formation of three to five molecular layers of NiO or $\text{Ni}(\text{OH})_2$. The formation of such layer causes the passivation of the electrode surface and determines the open-circuit potential, $E_{i=0}$ values of 0.7–0.8 V. As it has already been mentioned, literature data confirm the formation of the NiO or $\text{Ni}(\text{OH})_2$ phases on the Ni electrode surface in alkaline solutions [36, 40]. When

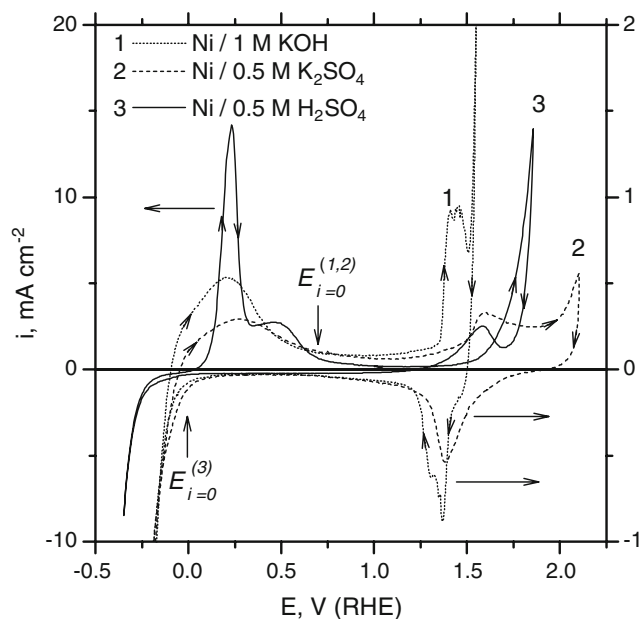
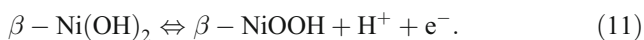


Fig. 2 Cyclic voltammograms of nickel electrode in 1 M KOH, 0.5 M K₂SO₄, and 0.5 M H₂SO₄ solutions, $\nu=50 \text{ mV s}^{-1}$, 20 °C, $E_{i=0}$ is the value of the open-circuit potential

such passive nickel electrode is anodized further in alkaline solution, two characteristic sharp increases in anodic current at ~1.35 and 1.5 V appear in the voltammograms (Fig. 2, curve 1). The first peak should be related to the oxidation of the Ni(II) surface compounds to Ni(III) because the charge corresponding to this current peak is about 2.2 mC cm^{-2} , which makes about half of the $Q_a^{(1)}$. According to Seghioeur et al. [35] and Wherens-Dijksma and Notten [39], the process at 1.35 V reflects the oxidation of ordered, compact $\beta\text{-Ni(OH)}_2$ phase to hydrous Ni(III) oxide, i.e., $\beta\text{-NiOOH}$ phase, the reversible reduction of which takes place at ~1.4 V, as can be seen from curve 1 (Fig. 2) [35]. This well-known process, used in Ni-based rechargeable alkaline batteries, is described by the equation:



The value of standard potential of reaction 11, estimated from curve 1 (Fig. 2), is $E^0=1.40\pm 0.02 \text{ V}$, which is close to the value reported in the revised Pourbaix diagram for nickel [38]. One can see that the shape of both anodic and cathodic peaks at ~1.4 V is irregular, reflecting some additional processes, which will be discussed later.

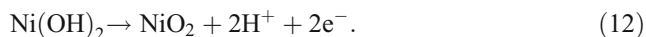
The anodic process at 1.5 V, observed in the solution of 1 M KOH (Fig. 2, curve 1), should be related to the further oxidation of surface Ni(III) compounds to Ni(IV) state, as $E_{\text{Ni}_2\text{O}_3/\text{NiO}_2}^0 = 1.434 \text{ V}$ [28]. In fact, however, OER takes place at $E > 1.5 \text{ V}$. In the cathodic part of cycle 1 (Fig. 2), at $E \approx 1.5 \text{ V}$, before the cathodic peak of NiOOH reduction, one can discern a small cathodic current wave with $Q_c \approx$

0.5 mC cm^{-2} , which could be related to the reduction of possible intermediate in O₂ evolution process or the so-called precursor of O₂ molecule. According to Wherens-Dijksma and Notten [39], upon oxidation above 1.4–1.5 V, the compact $\beta\text{-NiOOH}$ phase where the nickel oxidation state is 3, transforms into the dispersed $\gamma\text{-NiOOH}$ phase where the nickel oxidation state is 3.5–3.7. The value of nickel oxidation state higher than 3 is obtained when the anodic charge required for $\gamma\text{-NiOOH}$ formation is divided by the amount of nickel in the surface layer evaluated by means of various analytic techniques [30]. Thus, it becomes evident that the $\gamma\text{-NiOOH}$ phase represents the mix of NiOOH and other nickel compounds containing Ni in higher oxidation state. In the case of NiO₂, for instance, such mix would be composed of equal portions of NiOOH and NiO₂, i.e., NiOOH·NiO₂. According to Beverskog and Puigdomenech [38] and Barnard and Randell [44, 45], the composition of the $\gamma\text{-NiOOH}$ phase is $0.835 \text{ NiO}_2 \cdot 0.165 \text{ Ni(OH)}_2 \cdot 0.35 \text{ H}_2\text{O} \cdot 0.33 \text{ KOH}$, whereas $\beta\text{-NiOOH}$ is considered to be composed of $0.75 \text{ NiOOH} \cdot 0.25 \text{ Ni(OH)}_2 \cdot 0.22 \text{ H}_2\text{O} \cdot 0.025 \text{ KOH}$. As it will be discussed further, the above composition of the $\gamma\text{-NiOOH}$ phase could be possible in the case of neutral solutions, whereas in alkaline medium, nickel oxyhydroxide NiOOH should be the main component. It is known [31] that the formation of the $\gamma\text{-NiOOH}$ phase is the reason for the second low-voltage plateau at 0.8 V (RHE) in voltammetric response of alkaline batteries with nickel hydroxide positive electrodes. Such plateau could be determined by the hydrous Ni₃O₄·2H₂O phase [28], which can also be represented as Ni₂O₃·NiO·2H₂O or 2NiOOH·Ni(OH)₂ where the average nickel oxidation state is 2.66. This phase is thermodynamically stable within the E range from 0.8 to 1.2 V [28]. Some amount of it may be formed as a result of the chemical decomposition of the $\gamma\text{-NiOOH}$ phase, as will be shown further.

One can see that in the course of the electrochemical reduction of the $\gamma\text{-NiOOH}$ phase, the rate of reduction of the NiOOH component decreases significantly within the E range from 1.2 to 0.8 V (cathodic part of curve 1 in Fig. 2). This particular cathodic E range should be the region of the so-called $\alpha\text{-Ni(OH)}_2$ phase existence because the oxidation state of Ni in this phase varies between ~2.2 and 2.0 due to the incomplete reduction of NiOOH. At $E < 0.8 \text{ V}$, pure Ni(OH)₂ or the so-called $\beta\text{-Ni(OH)}_2$ should exist. Although the shape of the cathodic peak at ~1.4 V is irregular (curve 1), the above-indicated 2NiOOH·Ni(OH)₂ phase is not likely to form on the electrode surface because no indication of any reduction process is observed at 0.8 V in the voltammogram. After the complete reduction of the $\gamma\text{-NiOOH}$ phase at $E \approx 0.8 \text{ V}$, nickel remains passive in alkaline solution due to the recovery of the passivating layer on the electrode surface within the E range down to

0.25 V. Below this E value, the reduction of the passivating layer takes place with concomitant evolution of H_2 at $E \approx -0.1$ V. The main reason for the hydrogen evolution overvoltage, most likely, is the hardly reducible semiconducting monolayer of NiO, lying directly on the metal surface [4]. The amount of charge related to the reduction of this layer within the E range 0.25– -0.1 V is 0.6 to 0.8 $mC\ cm^{-2}$.

Curve 2 in Fig. 2 illustrates the electrochemical behavior of nickel in neutral solution of 0.5 M K_2SO_4 (pH 5.5). One can see that at $E < E_{i=0}^{1,2}$, there are no essential differences between voltammograms 1 and 2 in Fig. 2. The region of major divergence of these two curves is at $E > 1.3$ V. Instead of two sudden increases in anodic current, observed in 1 M KOH within 1.35–1.5 V (Fig. 2, curve 1), just slight, monotonic increase in anodic current is seen in neutral media. Such behavior, most likely, should be attributed to the absence of OH^- ions. At $E > 1.5$ V, the anodic current wave with a minimum at ~ 1.9 V is observed and followed by the beginning of the oxygen evolution process. The cathodic part of the voltammogram reveals a current peak of a regular shape, which is definitely different from the one described previously (Fig. 2, curve 1). The charge corresponding to the first anodic peak at $E < E_{i=0}^{1,2}$ is $Q_a^{(2)} \approx 3.2\ mC\ cm^{-2}$ and is almost the same as that of the anodic current wave at $E > 1.5$ V. Consequently, the anodic process reflected by the latter should also involve the transfer of two electrons related to the transformation of the $Ni(OH)_2$ layer into anhydrous NiO_2 according to the following reaction:



In such case, the cathodic current peak with charge Q_c also close to 3 $mC\ cm^{-2}$ should be attributed to the reduction of the NiO_2 layer. Comparison of the cathodic peaks of cycles 1 and 2 (Fig. 2) suggests that in the case of neutral solution reduction of the NiO_2 layer begins at ~ 1.8 V and up to $E_{max} = 1.4$ V the main product of reaction is the $O=Ni-OH$ phase, which is further reduced to $Ni(OH)_2$ as it has been described above in the case of curve 1 (Fig. 2). Because the cathodic peak of interest is of symmetric shape with respect to the peak potential $E_{max} = 1.4$ V, it is reasonable to suggest that up to 1.4 V whole amount of NiO_2 should be reduced to $NiOOH$. Thus, the formation and reduction of NiO_2 in neutral media proceeds in different ways. During the anodic process, at $E \approx 1.9$ V, a major part of the $Ni(OH)_2$ surface layer should be oxidized to NiO_2 and the composition of the surface layer should be close to 0.835 NiO_2 ·0.165 $Ni(OH)_2$ ·0.35 H_2O ·0.33 KOH [38] where the formal nickel oxidation state is ~ 3.5 . This mixture, however, cannot be identified as the γ - $NiOOH$ phase because it does not contain the $NiOOH$ component.

Figure 3 displays the cyclic voltammograms of the same system ($Ni/0.5\ M\ K_2SO_4$) with different values of anodic scan reversal potential. In cases when the scan is reversed at $E < 1.0$ V, small current wave appears in the voltammograms before the beginning of the H_2 evolution process. The comparison of the anodic and cathodic charges suggests that this current wave should be related to the reduction of compact passivating surface layer lying directly on the nickel surface. Reduction of the whole layer of $Ni(OH)_2$ formed during the anodic process becomes possible only after the reduction of this compact passivating layer and most likely takes place concomitantly with H_2 evolution. A certain part of this layer may dissolve in neutral electrolyte [46]. When the potential scan is reversed at $E > 1.0$ V, this current wave disappears pointing to some restructuring of passivating layer at higher anodic potentials in a consequence of which its reduction becomes even more difficult and is possible only in the region of hydrogen evolution. Cycle 3 in Fig. 3 shows that when the potential scan is reversed at 1.5 V, no cathodic current peak appears in the voltammograms at this range of potentials contrary to the case of Ni in 1 M KOH. The cathodic peak appears only after the oxidation of the Ni electrode at $E > 1.5$ V. The beginning of the NiO_2 reduction process also depends on the values of potential reached in the anodic scan.

Thermodynamically, the behavior of nickel in acidic electrolyte can be treated as the behavior of electronegative metal. The open-circuit potential of Ni in 0.5 M H_2SO_4 is $E_{i=0}^3 \sim 0$ V (Fig. 2, curve 3). The value of $E_{i=0}$ should be determined by the corrosion of nickel in acid under hydrogen depolarization conditions. In Podobaev and Reformatskaya [25], it has been suggested that at $E < 0$

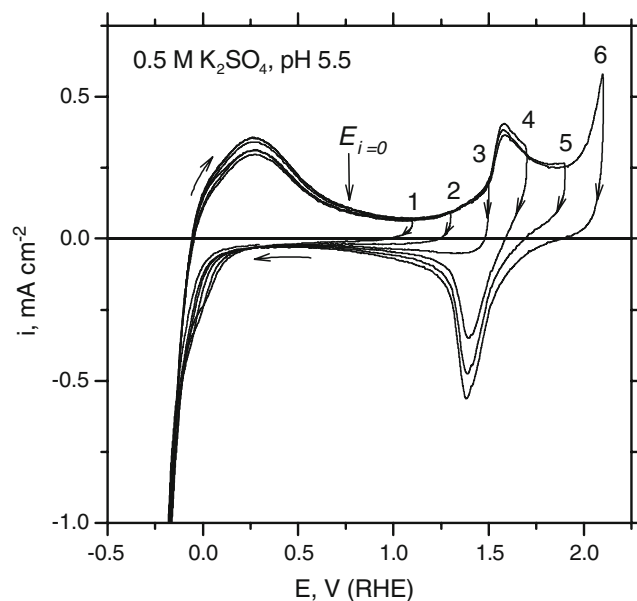


Fig. 3 Cyclic voltammograms of nickel electrode in 0.5 M K_2SO_4 , pH 5.5, $v = 50\ mV\ s^{-1}$, 20 °C

water molecules chemisorb on nickel surface with charge transfer of $0.8 e^-$ to form the surface complex in which the oxygen side of the H_2O dipole is most likely oriented towards the metal surface. Two characteristic anodic current peaks are observed in the E range from 0 to 1.0 V. The heights of these peaks and charge related to them depend on the experimental conditions and can vary in the wide range, which is evident from the comparison of voltammograms in Figs. 2 and 4. The rate of the anodic process within the E range of interest increases with the increase in solution acidity and also when nickel is activated in the H_2 evolution region. In the region of first anodic peak, i.e., at $E > 0$, active dissolution of the nickel phase with the formation of hydrated Ni^{2+} ions takes place, although thermodynamically this process should be possible at $E_{Ni^{2+}/Ni}^0 = -0.25 V$ [28]. The process most likely goes through the electrochemical stage of $Ni(OH)_2$ formation with subsequent dissolution of hydroxide in electrolyte. In the E range of the second anodic peak, passivation of nickel begins. This is evidenced by a minor cathodic current wave at $0.2 V > E > -0.2 V$ (Fig. 4), reflecting the reduction of the passivating layer. The charge related to this wave makes $\sim 0.8 mC cm^{-2}$, which is equivalent to the charge of one monolayer of O^{2-} ions or to the oxidation of one atomic layer of Ni to Ni^{2+} on the surface with roughness factor $f \approx 2$. When the Ni electrode is oxidized at 1.0 V–1.2 V, some restructuring and dehydration of the passivating layer occurs and its reduction becomes more difficult: cathodic current wave decreases, shifts towards more negative potentials till it becomes inseparable from the H_2 evolution process. A similar situation was observed in the case of Ni

in 0.5 M K_2SO_4 (Fig. 3). The main reason of nickel passivation in acid solution is most likely the formation of a hardly reducible, compact layer of NiO, which is also known to have p-type semiconductive properties [4]. Comparison of curves 1–3 in Fig. 2 in the vicinity of $E_{i=0}^{1,2}$ suggests that the passivation of the Ni electrode in acidic medium is stronger and the overvoltage of H_2 evolution is almost twice as large as in the case of neutral and alkaline media.

Anodic oxidation of the passivating NiO layer in the solution of 0.5 M H_2SO_4 begins at $\sim 1.3 V$ (Fig. 2, curve 3) and the product of this reaction, like in the case of neutral medium, is most likely NiO_2 . The process is accompanied by O_2 evolution, which begins at $E \approx 1.75 V$. When the potential scan is reversed in the OER region, anodic current wave appears in the negative-going scan at $1.7 V > E > 1.3 V$. The nature of this wave will be discussed further. Contrary to the case of neutral and alkaline solutions, no cathodic reduction process is observed within this particular range of potentials. At $E < 1.3 V$, the passivating layer of NiO should be recovered completely because hydrogen evolution begins at $\sim -0.2 V$ and there is no cathodic current wave preceding this process as described above (Fig. 4).

One can see from Fig. 2 that the OER on the surface of the Ni electrode in the solutions investigated takes place in different ranges of potential. This process is most easy in alkaline medium ($E \approx 1.5 V$). In the case of acidic solution, the OER begins at 1.75–1.8 V, i.e., almost precisely at $E_{H_2O_2/H_2O}^0 = 1.77 V$ where the direct oxidation of H_2O to H_2O_2 is thermodynamically possible [28]. In neutral medium (pH=5.5), the OER is most difficult, beginning at $\sim 2.0 V$. Thus, the potential of OER onset varies greatly in the solutions of interest, i.e., ΔE_{OER} makes $\sim 600 mV$.

Admitting the previously discussed possibility of peroxide-type compounds formation on the electrode surface, the mechanism of OER on nickel in alkaline solution could be explained by the sequence of following reactions:

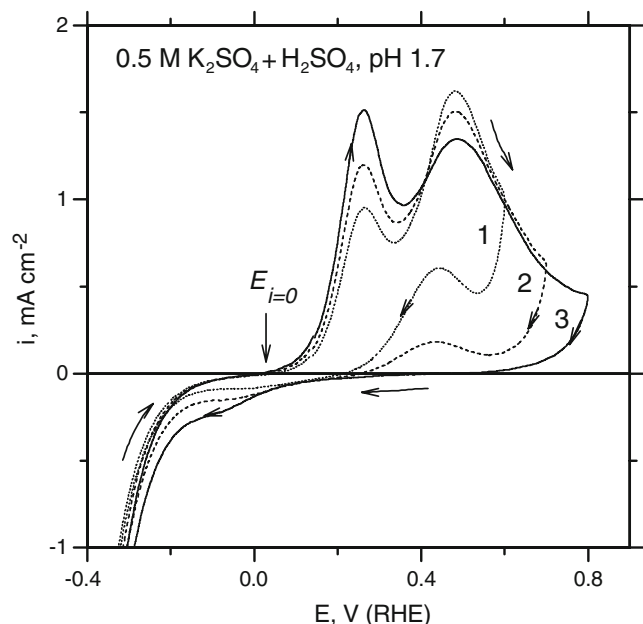
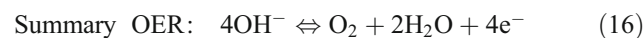
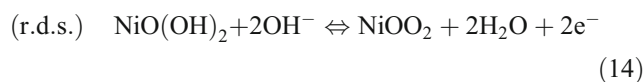
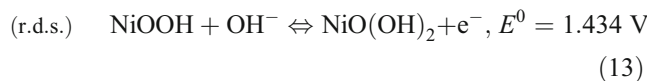
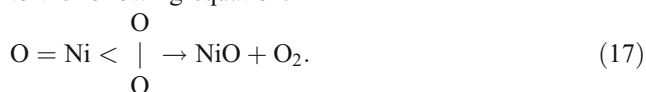


Fig. 4 Cyclic voltammograms of nickel electrode in 0.5 M $K_2SO_4 + H_2SO_4$, pH 1.7, $v = 50 mV s^{-1}$, $20^\circ C$

According to the above-presented scheme, the direct precursor of the O₂ molecule is Ni(IV) peroxide $\text{O} = \text{Ni} < \begin{array}{c} \text{O} \\ | \\ \text{NiOO}_2 \end{array}$ (Eq. 14), which forms in consequence of hydrous Ni(IV) oxide, NiO₂·H₂O, oxidation. Reactions 13 and 14 are reversible and, depending on certain conditions, should determine the overall rate of the process, whereas reaction 15 should be irreversible and fast. The main oxide, taking part in the overall process and playing the role of site, is hydrous Ni(III) oxide—NiOOH, which is fully recovered on the electrode surface after the sequence of reactions 13, 14, and 15. The formation of Ni(IV) peroxide on the electrode surface can be treated as the chemisorption of the O₂²⁻ ion, which is the reason of the above-mentioned depolarization of OER by ~300 mV with respect to $E_{\text{H}_2\text{O}_2/\text{H}_2\text{O}}^0$. One can see from Eqs. 13 and 14 that the transfer of three electrons is required for the formation of Ni(IV) peroxide from NiOOH, similar to the formation of NiOOH from Ni. Ascribing all electrons to nickel, its oxidation state in the NiOO₂ molecule would formally be +6. In the literature [28], hydrous Ni(IV) oxide is incorrectly considered as nickel peroxide. These are different compounds, however, as it follows from Eq. 14. Ni(IV) peroxide can decompose not only electrochemically reacting with OH⁻ (Eq. 15), but also chemically according to the following equation:

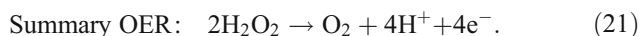
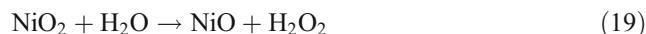
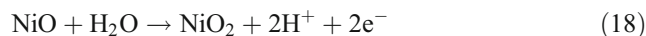


The above reaction may be the main reason of the indicated Ni₂O₃·NiO·2H₂O phase formation during the decomposition of the so-called γ-NiOOH phase.

The composition of nickel surface compounds at $E \approx 1.5$ V is reflected by the cathodic reduction profile in curve 1 (Fig. 2). One can see that the charge corresponding to the reduction of the Ni(IV) compounds within the E range from 1.5 to 1.4 V, reflected by the minor cathodic current wave, is ~0.5 mC cm⁻², whereas the charge consumed in the reduction of Ni(III) oxide within 1.4 V > E > 0.8 V is about 2.5 mC cm⁻². Thus, it follows that the γ-NiOOH phase, which forms on the Ni electrode surface in alkaline solution at ~1.5 V, i.e., in the range of OER, should be composed of ~5 parts of NiOOH and one part of nickel peroxide NiOO₂–5NiOOH·NiOO₂. The formal oxidation state of Ni in this mixed phase is ~3.5, which corresponds to the value reported in the literature [39]. So, the experiment confirms the above-suggested possibility of Ni(IV) peroxide formation on the electrode surface during the anodic process.

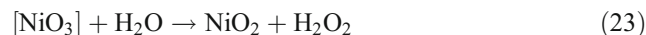
In the case of 0.5 M H₂SO₄, the role of the site for OER is played by the molecule of the passivating nickel oxide NiO, which is oxidized to NiO₂ in the course of the

process. In strongly acidic medium, NiO₂ is a strong oxidant, which is capable of oxidizing water to H₂O₂ ($E_{\text{Ni}^{2+}/\text{NiO}_2}^0 = 1.593 - 0.118 \text{ pH} - 0.029 c_{\text{Ni}^{2+}}$ [28]). The mechanism of OER on Ni in acid could be represented by the following sequence of reactions:



The anodic current peak at $E \approx 1.6$ V in the negative-going part of curve 3 in Fig. 2 can also serve as an argument confirming the possibility of NiO formation in the course of OER according to Eq. 19 and subsequent oxidation to NiO₂. The redox couple NiO₂/NiO (Eq. 19) acts as an electrocatalyst of H₂O oxidation to H₂O₂.

In neutral medium (0.5 M K₂SO₄, pH=5.5), anhydrous NiO₂ is stable within 1.5–1.9 V and passivates the nickel electrode surface (Figs. 2 and 3). NiO₂ should play the role of the site of OER in this case. Comparison of curves 2 and 3 in Fig. 2 shows that OER in neutral solutions takes place at an overvoltage of about 300 mV with respect to $E_{\text{H}_2\text{O}_2/\text{H}_2\text{O}}^0 = 1.77$ V. Because the direct oxidation of water molecules to OH radicals or O atoms should not be possible thermodynamically on the surface of NiO₂ at 2.0–2.1 V [28], it can be presumed that OER at such high anodic potential values is related to the further oxidation of NiO₂ to highly unstable Ni(VI) oxide NiO₃, which decomposes immediately as described by following equations:



The summary equation of OER is the same as Eq. 21. There are no data in the literature regarding NiO₃ oxide, however, oxidation number 6 is possible for metals of iron subfamily [28].

Thus, depending on the experimental conditions and actual state of the nickel electrode surface, three mechanisms of OER described by Eqs. 13, 14, 15, and 16; 18, 19, 20, and 21; and 22, 23, and 24 are possible. In all these cases, OER is an electrocatalytic process mediated by nickel surface oxygen compounds and not by direct electrochemical oxidation of water molecules as described by Eqs. 1, 2, 3, and 4 [2] or 5, 6, 7, and 8. A distinctive

feature of these mechanisms is the fact that synchronous oxidation of two O^{2-} ions to O_2 molecule takes place on the same surface site, i.e., the molecule of nickel oxide, which undergoes changes in the course of the process. As for the mechanism described by Eqs. 13, 14, 15, and 16, it is reasonable to suggest that the OER in this case takes place at underpotential conditions with respect to $E_{\text{H}_2\text{O}_2/\text{H}_2\text{O}}^0 = 1.77 \text{ V}$ due to the possibility of nickel peroxide formation according to Eq. 14.

Additional arguments in favor of underpotential formation of the chemisorbed O_2^{2-} ion on the nickel electrode surface can be found in the kinetics of OER on Ni. Majority of the studies is devoted to alkaline solutions [29, 47, 48]. The main feature of OER kinetics in alkali is very small slope $dE/dlgi$, which makes 40 to 60 mV in the beginning of the process, i.e., at overvoltage, η , of 150–300 mV and $i_a < 10 \text{ mA cm}^{-2}$. At higher overvoltage ($>350 \text{ mV}$), the $dE/dlgi$ increases up to 120–160 mV. It should be noted that the overvoltage for OER is calculated with respect to $E_{\text{O}_2/2\text{H}_2\text{O}}^0 = 1.23 \text{ V}$. At low overvoltage, the reaction order with respect to OH^- , n_{OH^-} is 2, whereas at high η values, $n_{\text{OH}^-} = 1$ [7]. It is considered [29] that small values of $dE/dlgi$ are observed in the case when the rate of the process is limited by the transfer of second electron (Eq. 2), and large ones when the rate-determining step is the transfer of the first electron (Eq. 1). It should be noted, however, that the $dE/dlgi$ slope values lower than 60 mV can only be attributed to reversible electrochemical process involving transfer of two electrons and taking place in the E range close to its equilibrium potential. The rate-determining step of the irreversible one-electron process, taking place at an overvoltage of 150–300 mV, cannot, in principle, be characterized by such $dE/dlgi$ values. In spite of the fact that OER on nickel in alkali takes place at $\sim 1.5 \text{ V}$, the existence of hypothetical OH_{ad} and O_{ad} particles on the electrode surface under quasiequilibrium Langmuir conditions [29] is not plausible.

From the above-suggested mechanism of OER in alkaline medium (Eqs. 13, 14, 15, and 16), it follows that in case when r.d.s. of the process is reaction 14, which proceeds reversibly in the vicinity of its equilibrium potential at $E \approx 1.5 \text{ V}$ and if c_{OH^-} and $c_{\text{NiO}(\text{OH})_2}$ are constant, the theoretic slope $dE/dlgi$ should be equal to the Nernst slope, i.e., $2.3RT/2F \approx 30 \text{ mV}$, as the process involves the transfer of two electrons. The order of reaction 14 with respect to OH^- ions, n_{OH^-} , is 2. In case when the r.d.s. of the oxygen evolution process is reaction 13, which proceeds reversibly, the theoretic value of slope $dE/dlgi$ would be $2.3RT/F \approx 60 \text{ mV}$, as the process involves the transfer of one electron, and $n_{\text{OH}^-} = 1$. With the increase in anodic potential, the rate of reaction 14 should increase and reaction 13 should become the rate-determining step. In case when this reaction proceeds irreversibly at high

overpotential, the theoretic value of slope should be $2.3RT/\beta F$, i.e., $\sim 120 \text{ mV}$, provided that the charge transfer coefficient is $\beta \approx 0.5$. It should be emphasized that the case under consideration deals with the kinetics of the surface process described by Eqs. 13, 14, 15, and 16, i.e., with the kinetics of electrocatalysis, and not the kinetics of direct H_2O oxidation.

Generally, the experimental values of $dE/dlgi$ are higher than theoretic ones because theoretic presumptions usually do not correspond to the actual experimental conditions. The values of $dE/dlgi \approx 40 \text{ mV}$ and $n_{\text{OH}^-} = 2$ reported in the literature [7, 29] can be treated as the kinetic evidence of the reversible surface process involving the transfer of two electrons.

Figure 5 displays the cyclic voltammograms of metallic Ni, metallic Ni heated at $400 \text{ }^\circ\text{C}$ for $\sim 30 \text{ min}$, and black nickel coatings on Ni and Ti in the solution of 1 M KOH within the E range from ~ 0.7 to $\sim 1.7 \text{ V}$, i.e., from $E_{i=0}$ to the O_2 evolution process. At $E_{i=0}$, the surface state, structure, and chemical composition of the surface oxide layer on all these electrodes may differ. The surface of the metallic Ni electrode should be covered with a passivating layer of $\text{NiO-Ni}(\text{OH})_2$ as discussed above. The surface oxide layer on thermally treated nickel should be composed mainly of NiO and Ni_2O_3 because $\text{Ni}(\text{OH})_2$ decomposes

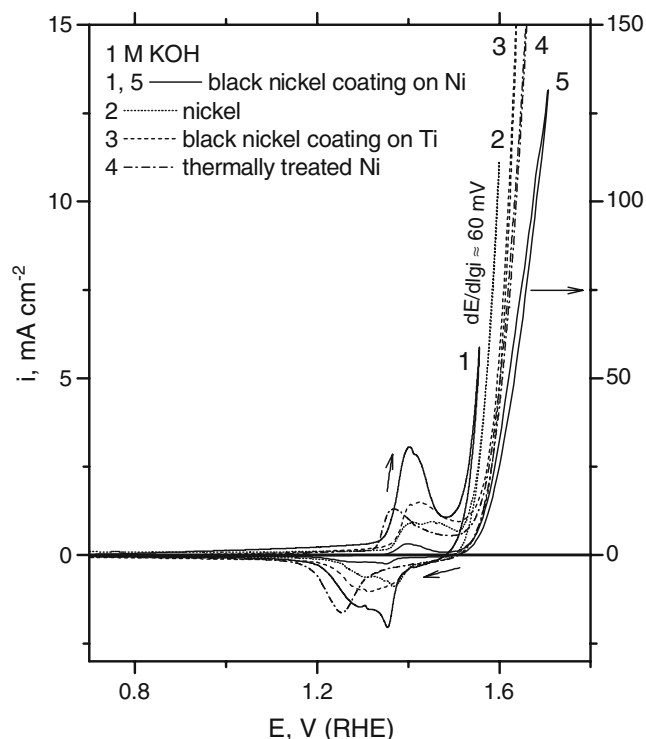


Fig. 5 Comparison of cyclic voltammograms of nickel, thermally treated nickel, and black nickel coatings on Ni and Ti substrates in 1 M KOH in oxygen evolution region, $\nu = 50 \text{ mV s}^{-1}$, $20 \text{ }^\circ\text{C}$

thermally at 230 °C to form NiO, which, in turn, oxidizes partly at ~400 °C to Ni₂O₃ [49]. The main component of the surface of black nickel coating should be Ni(OH)₂ as shown in Table 1. One can see that qualitatively the electrochemical behavior of all these electrodes within the *E* range preceding OER is very similar. A little bit different is the voltammogram of thermally treated Ni, which corresponds well with the curves of α-Ni(OH)₂ reported in Kim et al. [30] and Wherens-Dijksma and Notten [39]. In all cases (Fig. 5, curves 1–4), the anodic oxidation of NiO and Ni(OH)₂ to NiOOH begins almost at the same potential of ~1.35 V, whereas the cathodic reduction of anodic reaction products in the case of curve 4 is slightly hindered. In the beginning of the O₂ evolution process, the experimental slope *dE/dlgi* ranges between 50 and 60 mV, which corresponds to the literature values, although neither diffusion overvoltage constituent nor the error of potential measurement due to ohmic drop have been taken into account. At high current densities (Fig. 5, curve 5), *dE/dlgi* increases up to ~120 mV and more.

The above-discussed changes in nickel electrode surface state in alkaline, neutral, and acidic media in the *E* range preceding OER are schematized in Fig. 6. On the basis of these schemes, it can be concluded that pure Ni(OH)₂ and NiOOH phases are formed on nickel electrode in the course of anodic oxidation and they should correspond to β-Ni(OH)₂ and β-NiOOH phases described in the Bode and revised Pourbaix diagrams in Beverskog and Puigdomenech [38] and Wherens-Dijksma and Notten [39]. During the cathodic reduction of γ-NiOOH and NiO₂ phases in alkaline and neutral media, the α-Ni(OH)₂ phase [39] containing a small amount of NiOOH forms on the electrode surface within the *E* range from ~1.2 to ~0.8 V. On the basis of the electrochemical data, it has been inferred that the γ-NiOOH phase should be composed of the mixture of NiOOH and Ni(IV) peroxide NiOO₂ in the proportion ~5/6 NiOOH+~1/6NiOO₂ rather than ~5/6 NiO₂+~1/6 NiO as suggested in Beverskog and Puigdomenech [38].

Conclusions

1. The oxidation of water molecules, OH⁻ ions, or more precisely, O²⁻ ions to molecular oxygen on the surface of nickel oxide electrodes is an electrocatalytic process mediated by nickel surface oxygen compounds.
2. It has been suggested that in the case of strongly alkaline medium, the role of the intermediate or the precursor of the O₂ molecule is played by Ni(IV) peroxide NiOO₂, which forms and can be reduced on

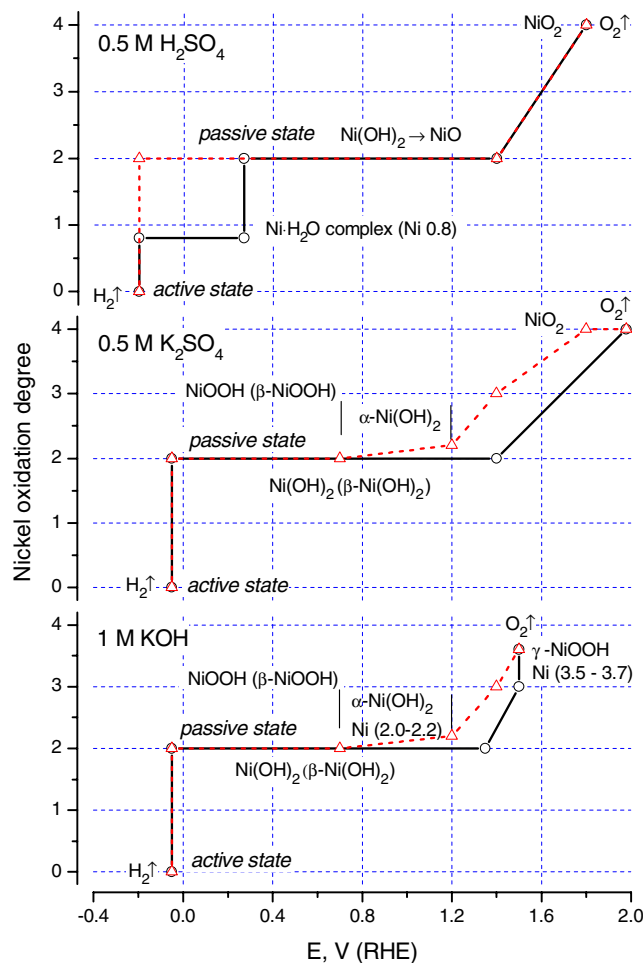
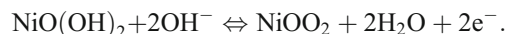


Fig. 6 Schematic representation of the redox processes taking place on the nickel electrode surface in the solutions of 1 M KOH, 0.5 M K₂SO₄, and 0.5 M H₂SO₄ in the course of anodic (circles) and cathodic (triangles) polarization

the electrode surface at *E* ≈ 1.5 V according to reversible electrochemical reaction as follows:



The formation of the Ni(IV) peroxide can be treated as the chemisorption of the O₂²⁻ ion, which, in turn, determines the underpotential (with respect to $E_{\text{H}_2\text{O}_2/\text{H}_2\text{O}}^0 = 1.77$ V), formation of O₂ molecule and, moreover, can explain the extremely small values of the *dE/dlgi* slope (40–60 mV) at low anodic current densities.

3. It has been presumed that in the case of OER on nickel in strongly acidic medium, H₂O₂ plays the role of O₂ precursor because the oxidation of water in this case takes place at $E \approx E_{\text{H}_2\text{O}_2/\text{H}_2\text{O}}^0$. The formation of H₂O₂ on the oxidized nickel surface is most likely to proceed according to the following reaction:



4. On the basis of the electrochemical data, it has been inferred that the composition of the γ -NiOOH phase should be $\sim 5/6$ NiOOH + $\sim 1/6$ NiOO₂ rather than $\sim 5/6$ NiO₂ + $\sim 1/6$ NiO as suggested in the literature.

References

- Trasatti S (1980) *Electrodes of conductive metallic oxides*, parts A, B. Elsevier, Amsterdam
- Matsumoto Y, Sato E (1986) *Mater Chem Phys* 14:397
- Krishtalik LI (1981) *Electrochim Acta* 26:329
- Shultze JW, Lohrengel MM (2000) *Electrochim Acta* 45:2499
- Jin S, Ye S (1996) *Electrochim Acta* 41:827
- Da Silva LA, Alves VA, Trasatti S, Boodts JFC (1997) *J Electroanal Chem* 427:97
- Wu G, Li N, Zhou D-R, Mitsuo K, Xu B-Q (2004) *J Solid State Chem* 177:3682
- Jirkovsky J, Markova M, Krtil P (2006) *Electrochem Commun* 8:1417
- Vazquez-Gomez L, Ferro S, De Battisti A (2006) *Appl Catal B Environ* 67:34
- Godinho MI, Catarino MA, Da Silva Pereira MI, Mendonca MH, Costa FM (2002) *Electrochim Acta* 47:4307
- Wang X, Luo H, Yang H, Sebastian PJ, Gamboa SA (2004) *Int J Hydrogen Energy* 29:967
- Chin B, Lin H, Li J, Wang N, Yang J (2006) *Int J Hydrogen Energy* 31:1210
- Aromaa J, Forsen O (2006) *Electrochim Acta* 51:6104
- Izumiya K, Akiyama E, Habazaki H, Kumagai N, Kawashima A, Hashimoto K (1997) *Mater Trans JIM* 38:899
- Corrigan DA (1987) *J Electrochem Soc* 134:377
- Corrigan DA, Bendert RM (1989) *J Electrochem Soc* 136:723
- Miller EL, Rocheleau RE (1997) *J Electrochem Soc* 144:1995
- Korovin NV, Kasatkin EV (1993) *Russ Electrochem* 29:448
- Sattar MA, Conway BE (1969) *Electrochim Acta* 14:695
- Conway BE, Sattar MA, Gilroy D (1969) *Electrochim Acta* 14:677
- Hoare JP (1968) *The electrochemistry of oxygen*. Wiley, New York
- Vetter KJ (1961) *Elektrochemische Kinetik*. Springer, Berlin
- Conway BE, Liu TC (1989) *Mater Chem Phys* 22:163
- Rossmel J, Qu Z-W, Zhu H, Kroes G-J, Norskov JK (2007) *J Electroanal Chem* 607:83
- Podobaev AN, Reformatkaya II (2006) *Prot Met* 42:73
- Oliveira PP, Patrito EM, Sellers H (1994) *Surf Sci* 313:25
- Bockris JO'M, Otagawa TJ (1984) *J Electrochem Soc* 131:290
- Pourbaix M (1963) *Atlas d'équilibres électrochimiques*. Gauthier-Villars, Paris
- Bronoel G, Reby J (1980) *Electrochim Acta* 25:973
- Kim M-S, Hwang T-S, Kim K-B (1997) *J Electrochem Soc* 144:1537
- Sac-Epee N, Palacin MR, Beaudoin B, Delahaye-Vidal A, Jamin T, Chabre Y, Tarascon J-M (1997) *J Electrochem Soc* 144:3896
- Lu PWT, Srinivasan S (1978) *J Electrochem Soc* 125:1416
- Corrigan DA, Knight SL (1989) *J Electrochem Soc* 136:613
- O'Grady WE, Pandya KI, Swider KE, Corrigan DA (1996) *J Electrochem Soc* 143:1613
- Seghioer A, Chevalet J, Barhoun A, Lantelme F (1998) *J Electroanal Chem* 442:113
- Medway SL, Lucas CA, Kowal A, Nichols RJ, Johnson D (2006) *J Electroanal Chem* 587:172
- Grden M, Klimek K (2005) *J Electroanal Chem* 581:122
- Beverkog B, Puigdomenech I (1997) *Corros Sci* 39:969
- Wherens-Dijkmsa M, Notten PHL (2006) *Electrochim Acta* 51:3609
- De Souza LMM, Kong FP, McLarnon FR, Muller RH (1997) *Electrochim Acta* 42:1253
- Brigs D, Seach MP (1987) *Practical surface analysis by Auger and X-ray photoelectron spectroscopy*. Mir, Moscow
- Wagner CD, Riggs WM, Davis LE, Moulder JF (1978) *Handbook of X-ray photoelectron spectroscopy*. Minnesota, Perkin-Elmer
- Wagner CD, Naumkin AV, Kraut-Vass A, Allison JW, Powell CJ, Rumble JR Jr (2000) NIST Standard Reference Database 20, Version 3.4 (Web Version)
- Barnard R, Randell CF, Tye FL (1980) *J Appl Electrochem* 10:109
- Barnard R, Randell CF (1982) *J Appl Electrochem* 12:27
- Gregori J, Garcia-Jareno JJ, Gimenez-Romero D, Vicente F (2006) *Electrochim Acta* 52:658
- Krasilshchikov AI (1963) *Zh Fiz Khim* 37:531
- Tsinman AI (1963) *Zh Fiz Khim* 37:273
- Hodgman ChD, Lange NA (1928) *Handbook of chemistry and physics*, 13th edn. The Norwood Press, USA